

Theoretical Investigation of the Role of Perfusion Rate and Haematocrit on Blood Flow and its Impact on Radiation Behavior of Tissue for Tumor Treatment

KW Bunonyo¹ and E. Amos²

Abstract

This research focused on the role of perfusion rate and haematocrit on blood flow by formulating nonlinear governing equations subject to some boundary conditions. The models were solved analytically using perturbation technique and the functions obtained for velocity and temperature were simulated using Mathematic 10 for velocity, temperature, wall shear stress, rate of heat transfer and volumetric flow rate by varying the resulting pertinent parameters, to see the influence on the flow profiles. It is noticed that Da, Rd, θ_w, Gr and R_T influenced the velocity positively while Cl, H, δ and M influenced the velocity negatively. Secondly, the parameters θ_w, Rd and R_T increase the temperature profile within the tumor and the enhancement of temperature above 316K for hyperthermia treatment in cancer therapy, while Cl, δ and α decreases the temperature profile. The aforementioned parameters also increase the volumetric flow rate and decrease the wall shear stress as well as the rate of heat transfer.

AMS Subject Classification: 58D30, 92B05.

Keywords: Perfusion rate, Wall Temperature, Tissue, Treatment, Tumor, Haematocrit, Blood.

¹ Department of Mathematics and Statistics, Federal University Otuoke, Nigeria.

² Department of Mathematics, Rivers State University Port Harcourt, Nigeria.

1. Introduction

Bio-magnetic fluid dynamics (BFD) is a new area in fluid mechanics study the fluid dynamics of biological fluids in the presence of applied magnetic field. A bio-magnetic fluid is a fluid of the living beings and its flow is influenced by the presence of magnetic field. The basic bio-magnetic fluid is blood, which behaves as a magnetic fluid, as stated by Higashi *et al.* [1] due to the complex interaction of the intercellular protein. The inhibitory effects of Lorentz force on the flow of blood in the presence of an atherosclerosis are (i) to reduce the high shear stress caused by atherosclerosis and hence to prevent the damage to the red and endothelial cells and (ii) to delay the transition from laminar to turbulent flow (Chandrasekhar [2]; Rudraiah [3]) inside the lumen and thus reducing high intensity shear area, which are unfavorable to the blood and arterial wall. Over the years, flow of biological fluids under the influence of a magnetic field has been investigated by several researchers due to its suspected applications in the field of bioengineering and medicine (Haik [4]; Ruuge [5]; Misra and Shit [6]).

Numerous researcher (Chaturani and Kaloni [7]; Chaturani and Upadhyya [8]; Shukla *et al.* [9]; Chaturani and Biswas [10]; Majhi and Usha [11]; Philip and Peeyush Chandra [12]) have theoretically studied the flow of blood through uniform and stenosed tubes and analyzed the influence of slip velocity or peripheral plasma layer thickness on the flow variables such as velocity and wall shear stress. In recent time, Tzirtzilakis [13], formulated a mathematical model of biomagnetic fluid dynamics to describe a Newtonian blood flow under the action of an applied magnetic field.

MHD flow through a channel with rigid boundaries are not of much use in understanding the characteristics of flow in arteries, because they are bounded by tissues which are idealized into a porous medium where one has to use a slip condition at the binding surface. It is important for the study of motion of contact line where the effective slip of the interface reverses the singularity in the rate of strain which was otherwise introduced by the no-slip condition. In the present situation the interface may be a smooth surface or a rough surface depending upon the solid matrix of the porous material.

In recent time, Ramakrishnan and Shailendra [14] analyzed the combined effects of Hartmann number and porous parameter on the steady flow in a channel of uniform width covered by porous media using BJ-slip condition. The BJ-slip condition is independent of the thickness of the porous layer and hence valid when the thickness of the porous layer is very much larger than the thickness of the fluid layer. In many industrial and biochemical applications the thickness of the porous layer is comparable to that of fluid layer and hence the slip condition should involve the thickness of the layer. Rudraiah [15] has derived the slip condition known as BJR slip condition involving the thickness of the layer. This BJR slip condition reduces to BJ condition for large thickness of the layer. Rudraiah *et al.* [16] investigated the electro-hydrodynamic dispersion of macromolecular components in a biological bearing using BJ and BJR slip conditions. Rudraiah *et al.* [17] studied

the electro-hydrodynamic dispersion of macromolecular components in a biological bearing consisting of a poorly conducting synovial fluid both in the cavity of the bones and in the bounding porous cartilage of finite thickness using BJR slip condition. Electro-hydrodynamic dispersion due to pulsatile flow in a channel bounded by porous layer of smart material was studied by Ng *et al.* [18] using both BJ and BJR slip conditions.

This present research is being motivated by studying the flow and heat transfer in branching tissues with tumor, the perfusion rate and haematocrit contribution to the flow behavior, and the useful application in clinical sciences, in particular in thermal therapy. It is significant in different problems of biomedical engineering and finds some important applications in various industrial manufacturing processes involving heat transfer. The theoretical study and varying parameters appropriately and estimating different parameters in controlling various problems of manufacturing industries can be achieved. Thus, this study is useful.

2. Mathematical formulation

Unsteady, laminar, highly viscous, conducting, hydromagnetic blood flow through a straight micro channel with permeable walls covered by porous media of finite thickness is considered. It is well known that at high shear rates blood behaves like a Newtonian fluid during flows through large blood vessels (Shivakumar *et al.* [19]; Misra *et al.* [20]; Copley [21]), Bunonyo *et al.* [22] investigated blood flow in arterial segment with heat transfer, and found the usefulness of some of the important parameters in controlling the flow behaviors and is very useful for clinicians. MacDonald [23] remarked that for vessels of radius greater than 0.025cm, blood may be considered as a homogeneous Newtonian fluid. Here we assume that blood behaves like a homogeneous conducting Newtonian fluid, with constant density ρ , viscosity μ and electrical conductivity σ . Further, it is well known fact that blood flow in arteries is pulsatile Burton [24]. Consider a Cartesian coordinate system (x^*, y^*) where x^* lies along the center of the channel, y^* is the distance measured in the normal section such that $y^* = R$ is the channel's half width. Let w^* be the velocity components in the directions of x^* . Then, the Navier-Stokes equations governing the flow are:

$$\rho \frac{\partial w^*}{\partial t^*} = -\frac{\partial P^*}{\partial x^*} + \mu^* \frac{\partial^2 w^*}{\partial y^{*2}} + \rho g \beta_c (T_t^* - T_a) - \frac{\mu^*}{k^*} w^* - \sigma B_0^2 w^* \quad (1)$$

$$\rho_t c_p \frac{\partial T_t^*}{\partial t^*} = k_t \frac{\partial^2 T_t^*}{\partial y^{*2}} - W_b C_b (T_t^* - T_a) + Q_H (T_t^* - T_a) \quad (2)$$

The corresponding boundary conditions are as:

$$\left. \begin{aligned} w^* = 0 \quad T_t^* = T_a \quad \text{at} \quad y^* = 0 \\ w^* = 0 \quad T_t^* = T_w \quad \text{at} \quad y^* = R \end{aligned} \right\} \quad (3)$$

The geometry of the tumor is given as follows:

$$y^*(x) = R_0 - \frac{\delta^*}{2} \left(1 + \cos 2 \frac{\pi x^*}{\lambda} \right) \quad (4)$$

where: λ is the length of the tumor, R_0 is the radius of normal tissue, δ^* is the height of the tumor, T_a is the blood temperature, T_t is the arterial temperature, T_w is the wall temperature, and R is the radius of abnormal tissue due to tumor growth.

We introduce the following non-dimensional conditions as:

$$\left. \begin{aligned} x = \frac{x^*}{\lambda}; y = \frac{y^*}{R_0}; w = \frac{w^* \mu_0}{w_0}; t = \omega t^*; P = \frac{P^* R_0}{w_0}; Da = \frac{k^*}{R_0^2}; Gr = \frac{g B_T T_a R_0^2}{\nu_0 w_0}; C_l = \frac{W_b C_b R_0^2}{k_b} \\ \theta = \frac{T_t^* - T_a}{T_a}; M = \frac{\sigma B_0^2 R_0^2}{\mu_0}; Rd = \frac{Q_H R_0^2}{\mu_0 c_p}; Pr = \frac{\mu_0 c_p}{k_t}; \alpha^2 = \frac{R_0^2 \omega}{\nu_0}; \mu = \frac{\mu^*}{\mu_0}; \delta^* = \frac{\delta R_0}{R_T} \end{aligned} \right\} \quad (5)$$

Using the dimensionless parameters in equation (5), we can simplify equations (1) and (2) as:

$$\alpha_1 \frac{\partial w}{\partial t} = -P_1 + \frac{\partial^2 w}{\partial y^2} - Da_1 w - Mw + Gr_1 \theta \quad (6)$$

$$\alpha^2 Pr \frac{\partial \theta}{\partial t} = \frac{\partial^2 \theta}{\partial y^2} - C_l \theta + Rd Pr \theta \quad (7)$$

$$\text{where: } \left. \begin{aligned} \alpha_1 &= \frac{\alpha^2}{(1+2.5H)}; P_1 = -\frac{P_0}{(1+2.5H)}; Da_1 = \frac{1}{Da(1+2.5H)}; \\ M &= \frac{M^2}{(1+2.5H)}; Gr_1 = \frac{Gr}{(1+2.5H)} \end{aligned} \right\}$$

Equation (6) and (7) are subject to the following boundary conditions:

The corresponding boundary conditions are as:

$$\left. \begin{aligned} w = 0 \quad \theta = 0 \quad \text{at} \quad y = 0 \\ w = 0 \quad \theta = \theta_w - 1 \quad \text{at} \quad y = h \end{aligned} \right\} \quad (8)$$

The geometry of the tumor is given as follows:

$$y(x) = 1 - \frac{\delta}{2R_T} (1 + \cos 2\pi x) \quad (9)$$

$$\text{where: } x = d_0 + \frac{\lambda}{2}$$

3. Method of solution

In order to solve equation (6) and (7) subject to the boundary condition (8), we adopt the solution in the following form:

$$\left. \begin{aligned} w &= w_0 e^{i\omega t} \\ \theta &= \theta_0 e^{i\omega t} \end{aligned} \right\} \quad (10)$$

Substitute equation (10) into (6) and (7), we have the following:

$$\frac{\partial^2 w_0}{\partial y^2} - (Da_1 + M + \alpha_1 i\omega) w_0 = P_1 - Gr_1 \theta_0 \quad (11)$$

$$\frac{\partial^2 \theta_0}{\partial y^2} - (C_l + \alpha^2 Pr \omega i - RdPr) \theta_0 = 0 \quad (12)$$

The corresponding boundary conditions are as:

$$\left. \begin{aligned} w_0 = 0, \quad \theta_0 = 0 & \quad \text{at } y = 0 \\ w_0 = 0, \quad \theta_0 = (\theta_w - 1)e^{-i\omega t} & \quad \text{at } y = h \end{aligned} \right\} \quad (13)$$

Let's apply the transformation: $\chi = \frac{y}{h}$ so that equation (11), (12) and (13) are transformed as:

$$\frac{\partial^2 w_0}{\partial \chi^2} - h(Da_1 + M + \alpha_1 i\omega)w_0 = hP_1 - hGr_1\theta_0 \quad (14)$$

$$\frac{\partial^2 \theta_0}{\partial \chi^2} - h(C_l + \alpha^2 Pr\omega i - RdPr)\theta_0 = 0 \quad (15)$$

The corresponding boundary conditions are as:

$$\left. \begin{aligned} w_0 = 0, \quad \theta_0 = 0 & \quad \text{at } \chi = 0 \\ w_0 = 0, \quad \theta_0 = (\theta_w - 1)e^{-i\omega t} & \quad \text{at } \chi = 1 \end{aligned} \right\} \quad (16)$$

Let $\beta_1 = h(Da_1 + M + \alpha_1 i\omega)$ and $\beta_2 = h(C_l + \alpha^2 Pr\omega i - RdPr)$, so that equation (14) and (15) are transformed as:

$$\frac{\partial^2 w_0}{\partial \chi^2} - \beta_1 w_0 = hP_1 - hGr_1\theta_0 \quad (17)$$

$$\frac{\partial^2 \theta_0}{\partial \chi^2} - \beta_2 \theta_0 = 0 \quad (18)$$

Solving equation (18) using the boundary condition equation (16), we obtain the following solution:

$$\theta_0(\chi) = \left(\frac{(\theta_w - 1)e^{-i\omega t}}{\sinh(\sqrt{\beta_2})} \right) \sinh(\sqrt{\beta_2}\chi) \quad (19)$$

Substitute equation (19) into equation (17) and solve:

$$\frac{\partial^2 w_0}{\partial \chi^2} - \beta_1 w_0 = P_2 - \beta_3 \sinh(\sqrt{\beta_2} \chi) \quad (20)$$

where: $\beta_3 = \left(\frac{hGr_1(\theta_w - 1)e^{-i\omega t}}{\sinh(\sqrt{\beta_2})} \right)$ and $P_2 = hP_1$

Equation (20) has a homogenous solution as:

$$w_{0h} = A \sinh(\sqrt{\beta_1} \chi) + B \cosh(\sqrt{\beta_1} \chi) \quad (21)$$

The particular solution is in the form:

$$w_{0p} = -\frac{P_2}{\beta_1} + \left(\frac{\beta_3}{\beta_1 - \beta_2} \right) \sinh(\sqrt{\beta_2} \chi) \quad (22)$$

The general solution of equation (20) is the sum of (21) and (22) as follows:

$$w_0 = A \sinh(\sqrt{\beta_1} \chi) + \left(\frac{P_2}{\beta_1} \right) \cosh(\sqrt{\beta_1} \chi) - \frac{P_2}{\beta_1} + \left(\frac{\beta_3}{\beta_1 - \beta_2} \right) \sinh(\sqrt{\beta_2} \chi) \quad (23)$$

We can now solve for the function coefficients in equation (23) using the boundary condition in equation (16) as:

$$A = \left(\frac{\beta_3}{\beta_2 - \beta_1} \right) \frac{\sinh(\sqrt{\beta_2})}{\sinh(\sqrt{\beta_1})} - \left(\frac{P_2}{\beta_1} \right) \frac{\cosh(\sqrt{\beta_1})}{\sinh(\sqrt{\beta_1})} + \frac{P_2}{\beta_1 \sinh(\sqrt{\beta_1})} \quad (24)$$

Substitute equation (23) and equation (19) into equation (10) as:

$$\theta(\chi) = \left(\frac{(\theta_w - 1)}{\sinh(\sqrt{\beta_2})} \right) \sinh(\sqrt{\beta_2} \chi) \quad (25)$$

$$w(\chi, t) = \left(A \sinh(\sqrt{\beta_1} \chi) + \left(\frac{P_2}{\beta_1} \right) \cosh(\sqrt{\beta_1} \chi) - \frac{P_2}{\beta_1} + \left(\frac{\beta_3}{\beta_1 - \beta_2} \right) \sinh(\sqrt{\beta_2} \chi) \right) e^{i\omega t} \quad (26)$$

The Rate of heat transfer is calculated from the temperature profile, it is obtained as:

$$Nu = \left(\frac{\sqrt{\beta_2} (\theta_w - 1)}{h \sinh(\sqrt{\beta_2})} \right) \cosh(\sqrt{\beta_2}) \quad (27)$$

The shear stress is calculated from the velocity profile, it is obtained as:

$$\tau_w = \left(\frac{A\sqrt{\beta_1}}{h} \cosh(\sqrt{\beta_1}) + \left(\frac{P_2\sqrt{\beta_1}}{h\beta_1} \right) \sinh(\sqrt{\beta_1}) + \left(\frac{\beta_3\sqrt{\beta_2}}{h(\beta_1 - \beta_2)} \right) \cosh(\sqrt{\beta_2}) \right) e^{i\omega t} \quad (28)$$

The volumetric flow rate is calculated from the velocity profile with the following result:

$$Q = \left(\begin{aligned} & \left(\frac{Ah}{\sqrt{\beta_1}} \cosh(\sqrt{\beta_1}) + \left(\frac{P_2h}{\beta_1\sqrt{\beta_1}} \right) \sinh(\sqrt{\beta_1}) - \frac{P_2h}{\beta_1} \right. \\ & \left. + \left(\frac{\beta_3h}{\sqrt{\beta_2}(\beta_1 - \beta_2)} \right) \cosh(\sqrt{\beta_2}) - \frac{Ah}{\sqrt{\beta_1}} - \left(\frac{\beta_3h}{\sqrt{\beta_2}(\beta_1 - \beta_2)} \right) \right) e^{i\omega t} \end{aligned} \right) \quad (29)$$

4. Results presentation

This section presents the graphical results of the analytical solutions in equation (25), (26), (27), (28) and equation (29) after carrying out numerical simulation by varying some of the pertinent parameters such as: $\theta_w = 1, Rd = 3, Gr = 10, H = 0.2, \delta = 0.3, R_T = 1.2, \alpha = 0.3, x = 0.3, Pr = 21, M = 3, Cl = 0.3$. On the basis of experiment investigations, Valvano *et al* [25] and Chato [26] reported the following data for human blood at a temperature $T = 310^\circ K$, $\mu = 3.2 \times 10^{-3} kg/ms, c_p = 14.65 J/kg^\circ K, k_b = 2.2 \times 10^{-3} J/ms^\circ K, \rho = 1050 kg/m^3$,

and hence $Pr = \frac{\mu c_p}{k_b} = 21$.

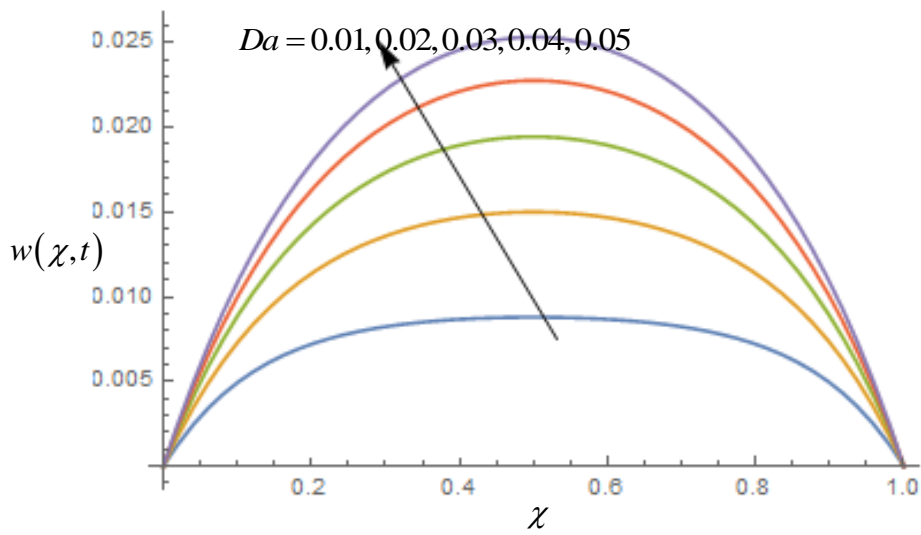


Figure 1: Influence of Da values on velocity profile

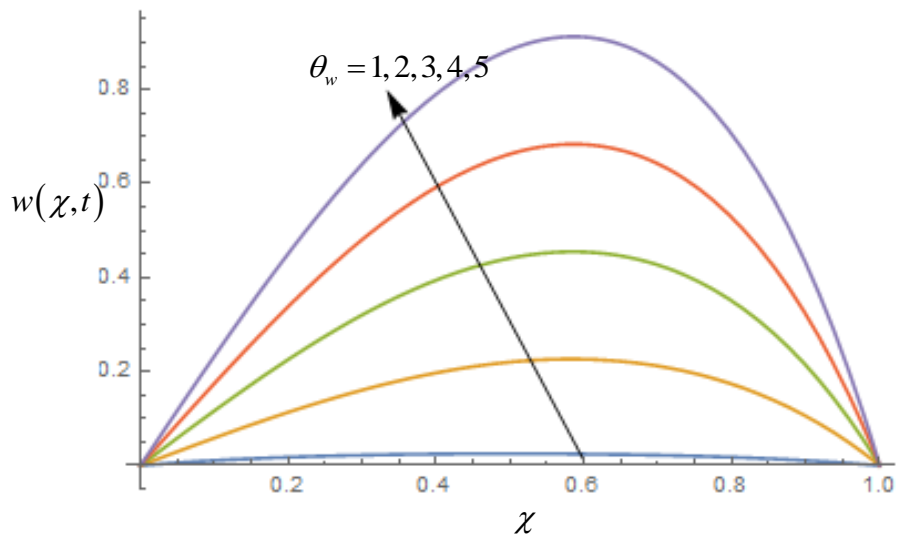


Figure 2: Influence of θ_w values on velocity profile

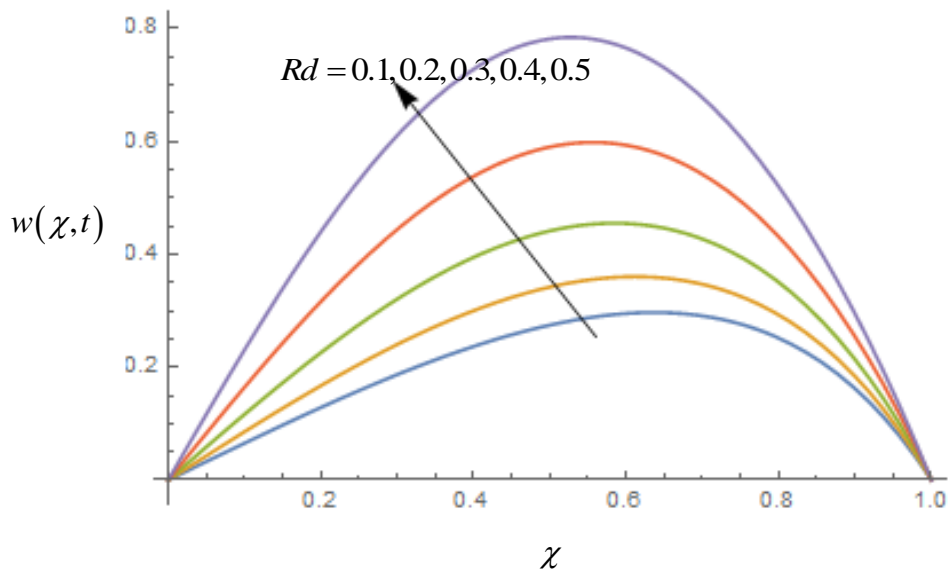


Figure 3: Influence of Rd values on velocity profile

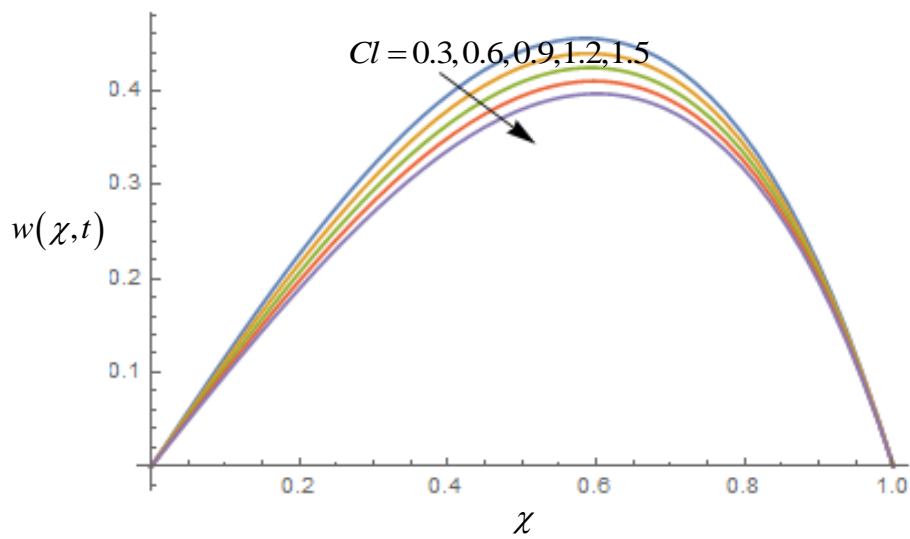


Figure 4: Influence of Cl values on velocity profile

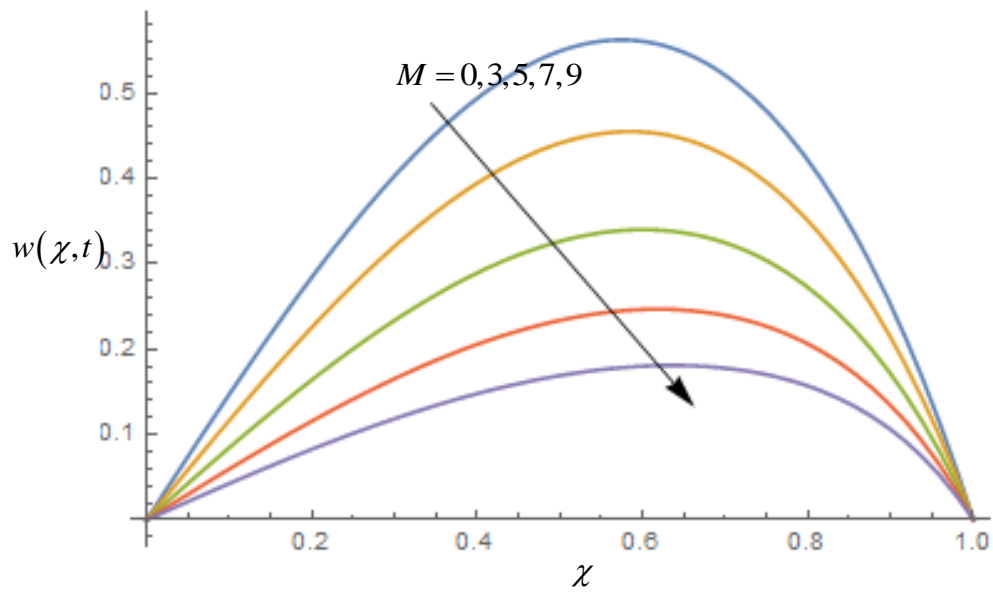


Figure 5: Influence of M values on velocity profile

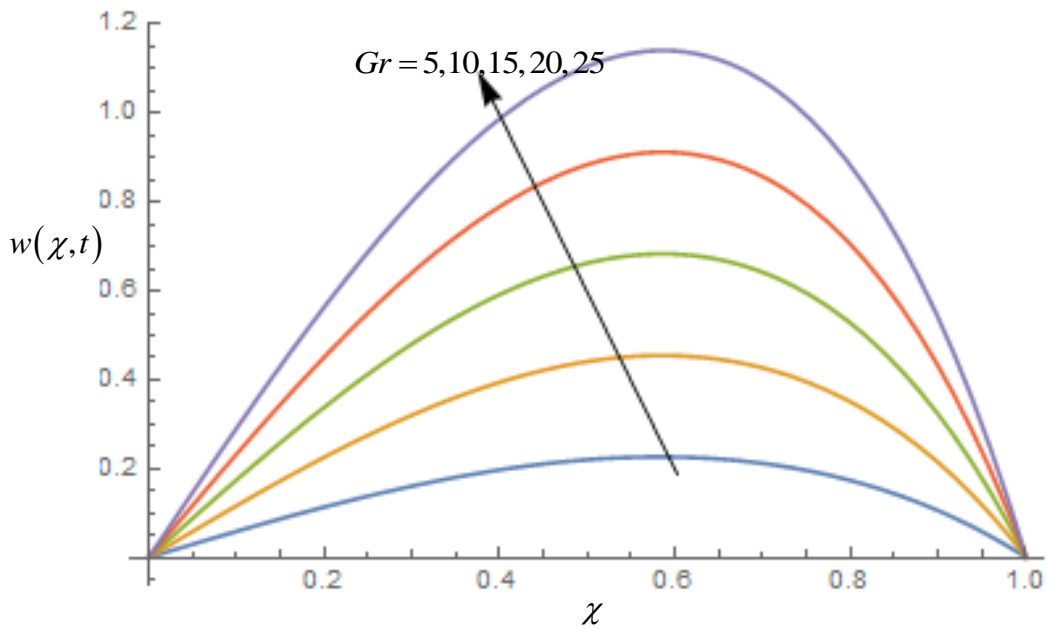


Figure 6: Influence of Gr values on velocity profile

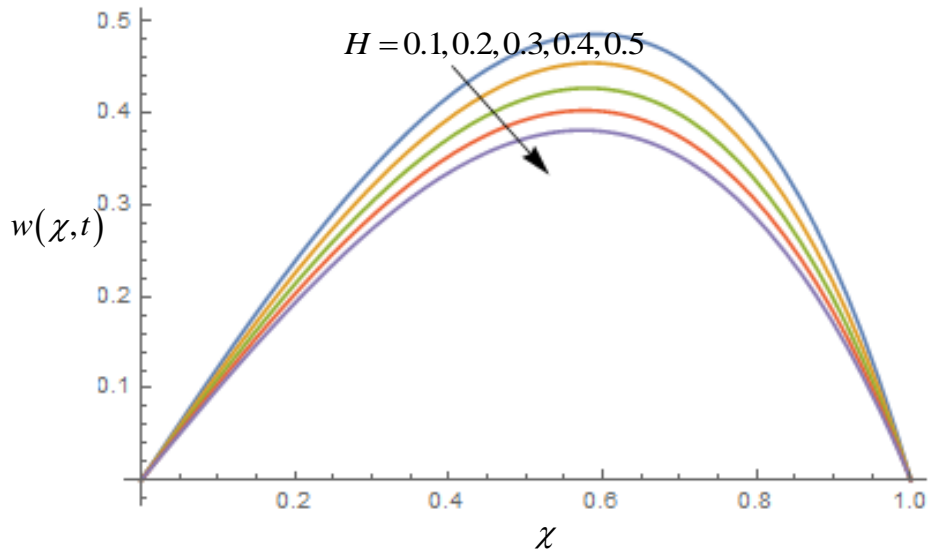


Figure 7: Influence of H values on velocity profile

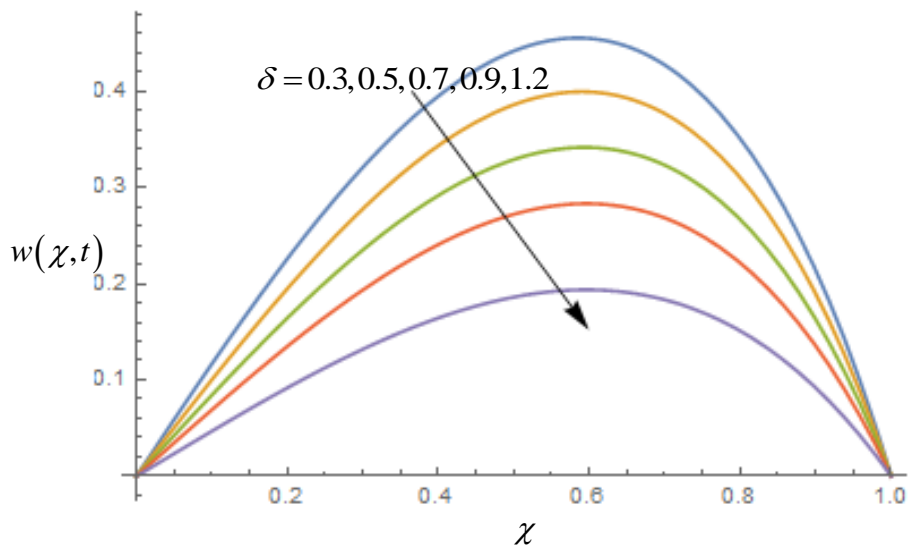


Figure 8: Influence of δ values on velocity profile

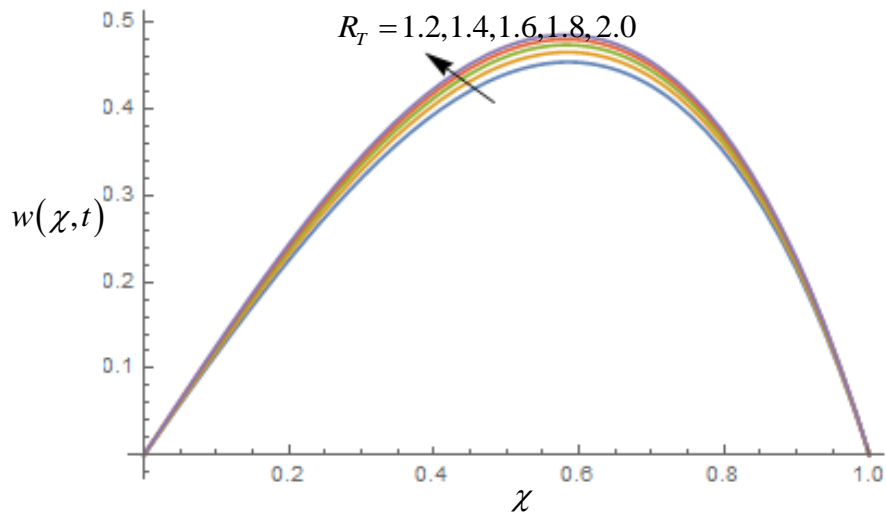


Figure 9: Influence of R_T values on velocity profile

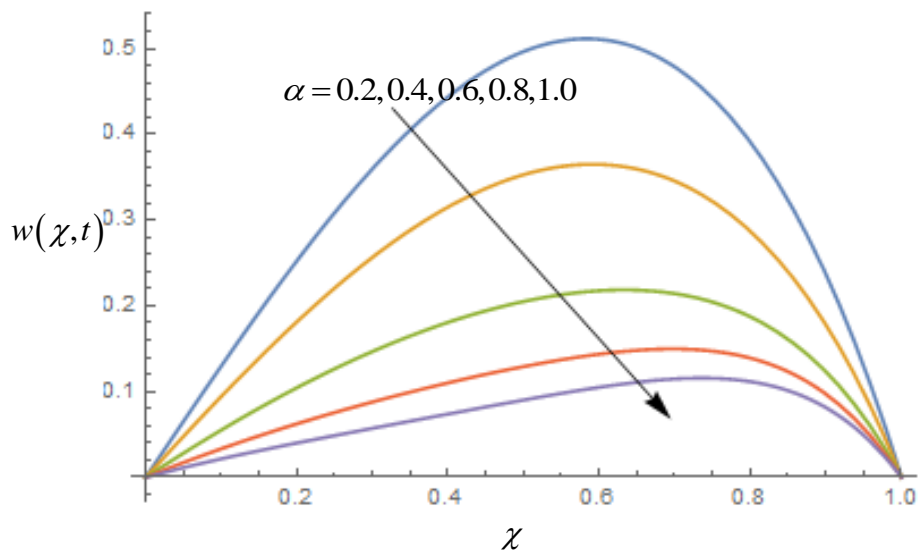


Figure10: Influence of α on velocity profile

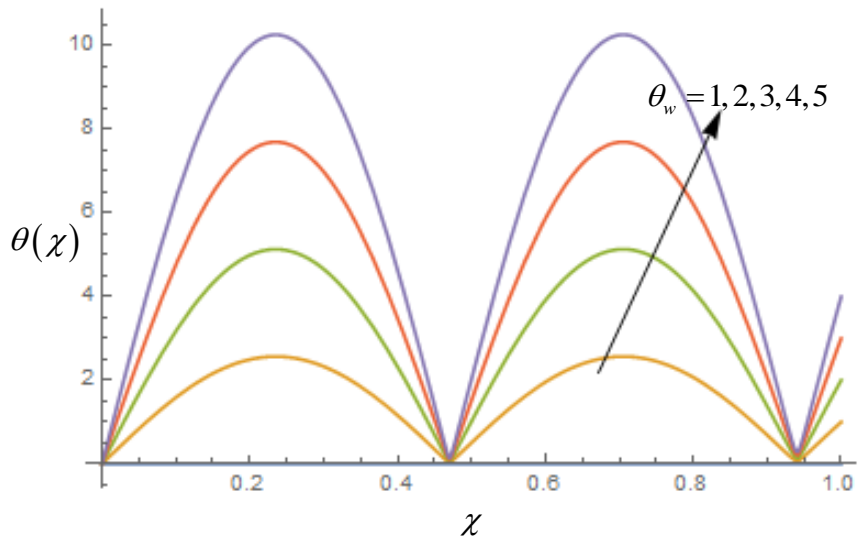


Figure 11: Influence of θ_w values on temperature profile

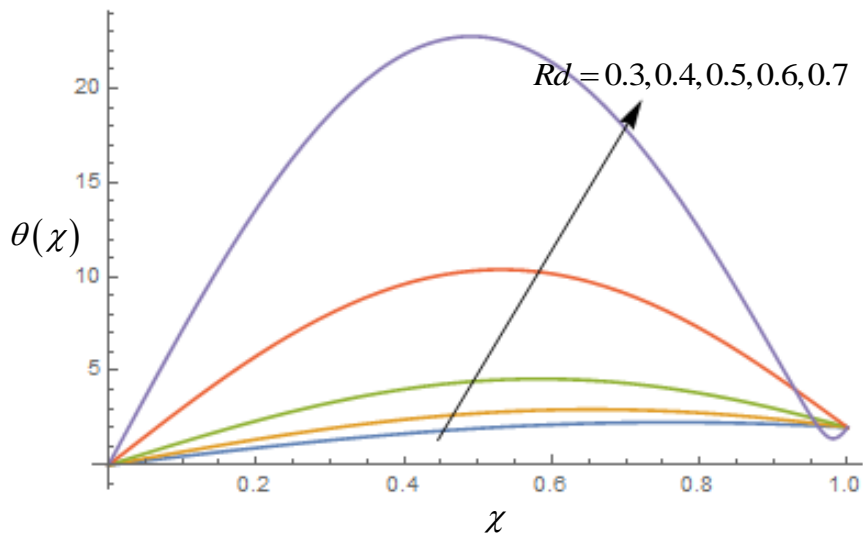


Figure 12: Influence of Rd values on temperature profile

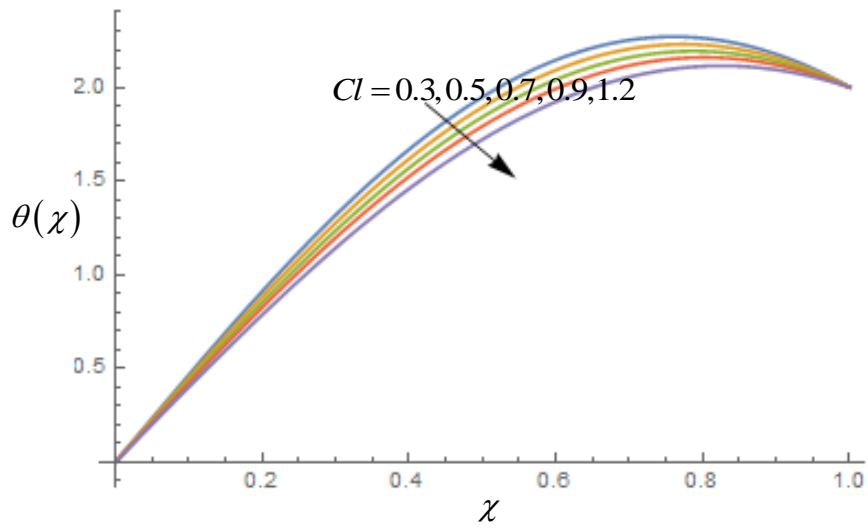


Figure 13: Influence of Cl values on temperature profile

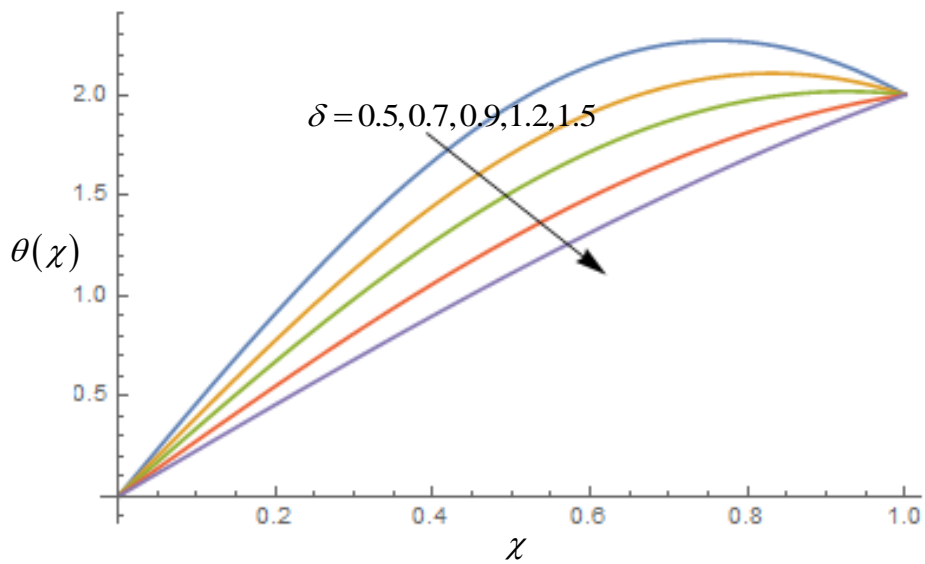


Figure 14: Influence of δ values on temperature profile

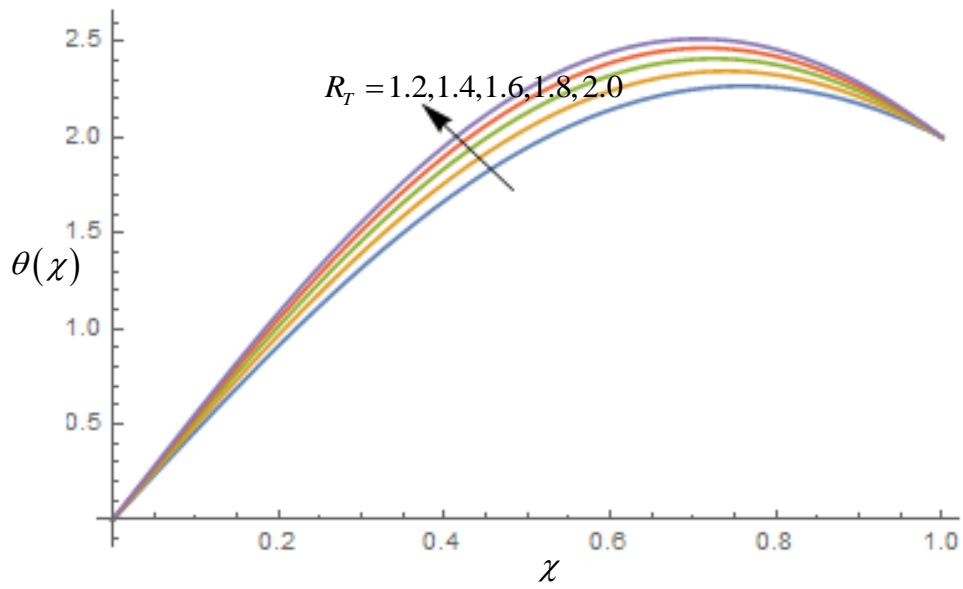


Figure 15: Influence of R_T values on temperature profile

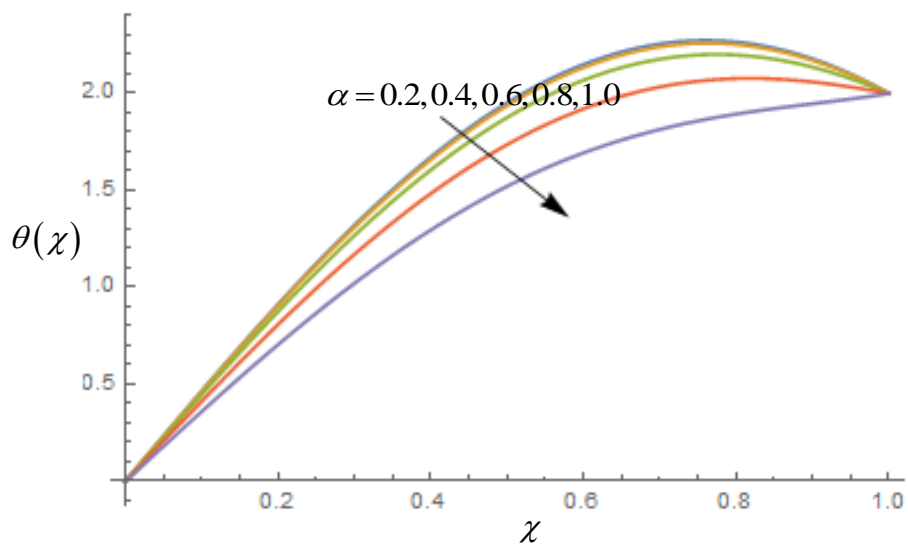


Figure 16: Influence of α values on temperature profile

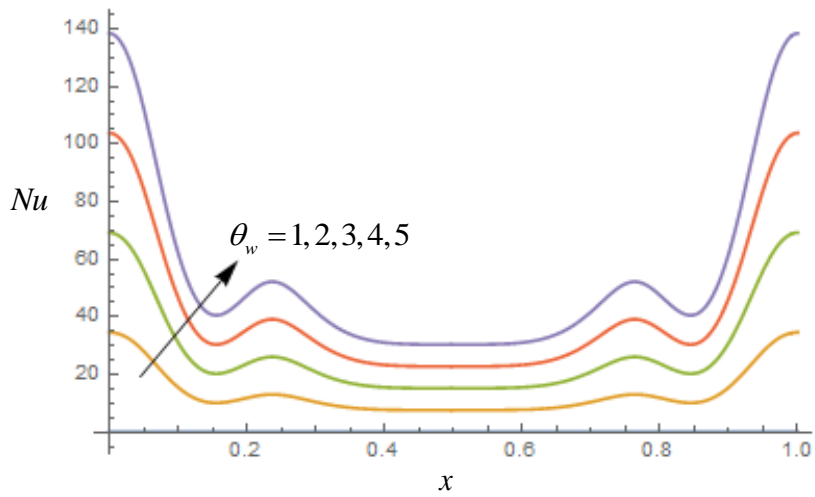


Figure 17: Effect of Rd values on Nusselt Number along the stenosed region

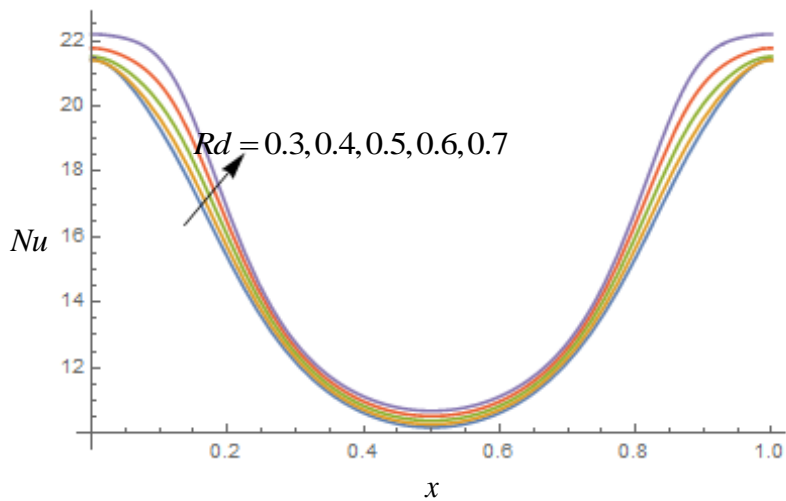


Figure 18: Effect of Rd values on Nusselt Number along the stenosed region

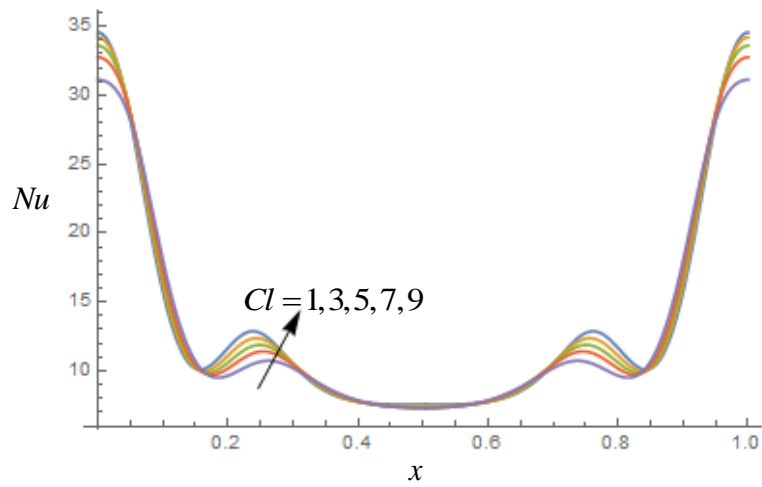


Figure 19: Effect of Cl values on Nusselt Number along the stenosed region

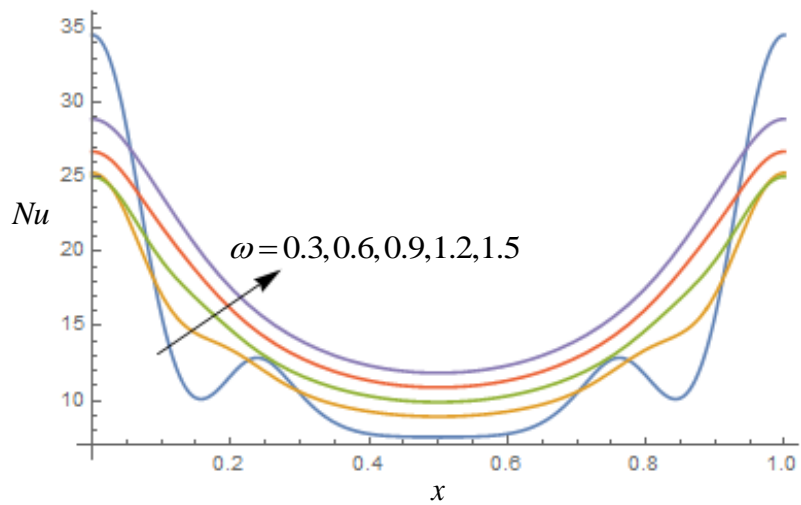


Figure 20: Effect of ω values on Nusselt Number along the stenosed region

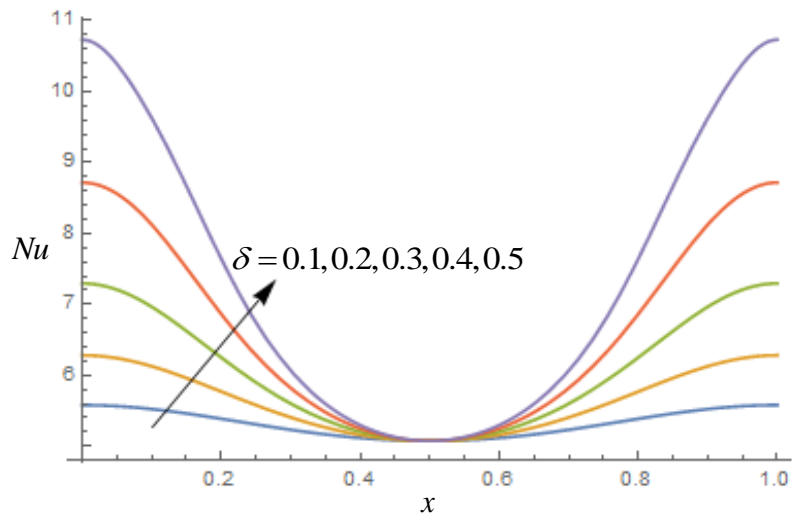


Figure 21: Effect of δ values on Nusselt Number along the stenosed region

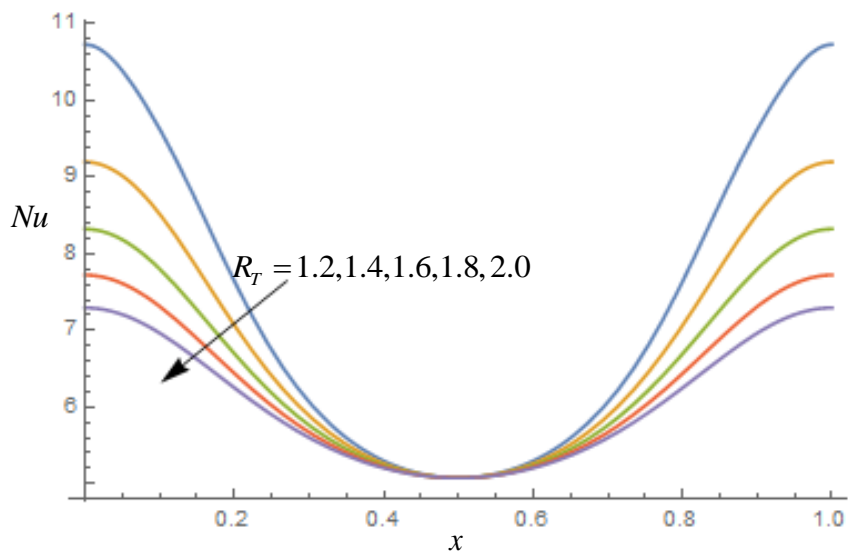


Figure 22: Effect of R_T values on Nusselt Number along the stenosed region

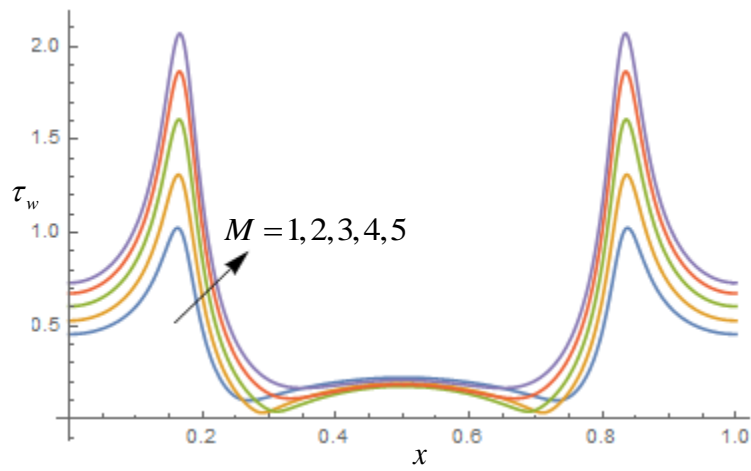


Figure 23: Effect of M values on Shear Stress along the stenosed region

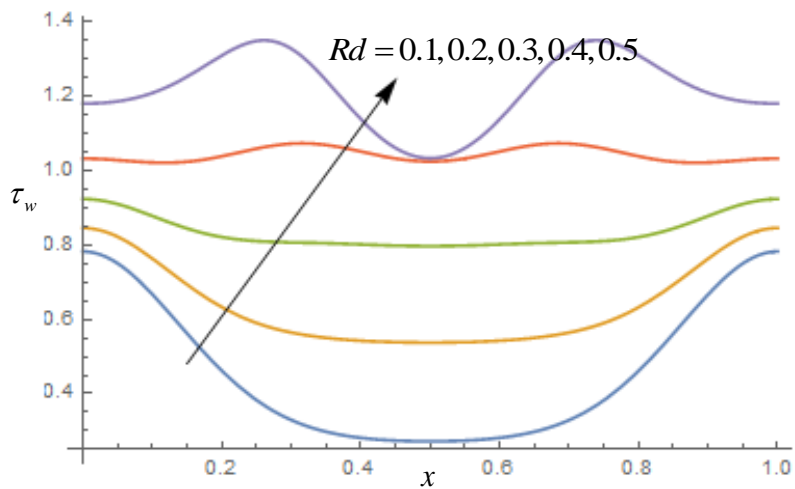


Figure 24: Effect of Rd values on Shear Stress along the stenosed region

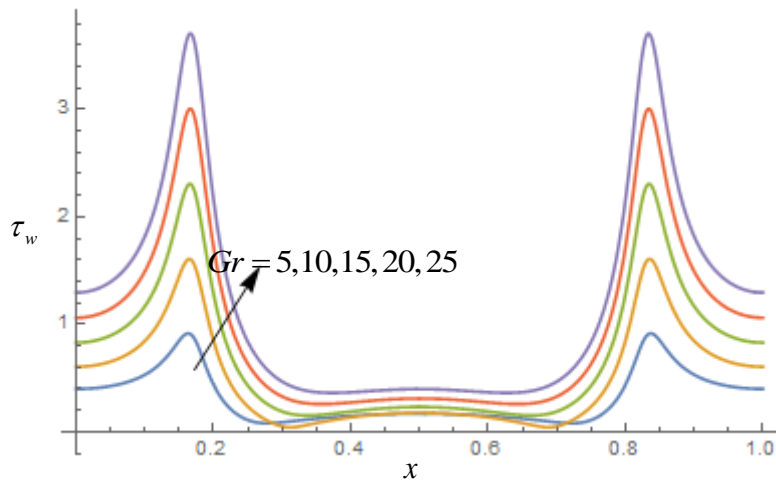


Figure 25: Effect of Gr values on Shear Stress along the stenosed region

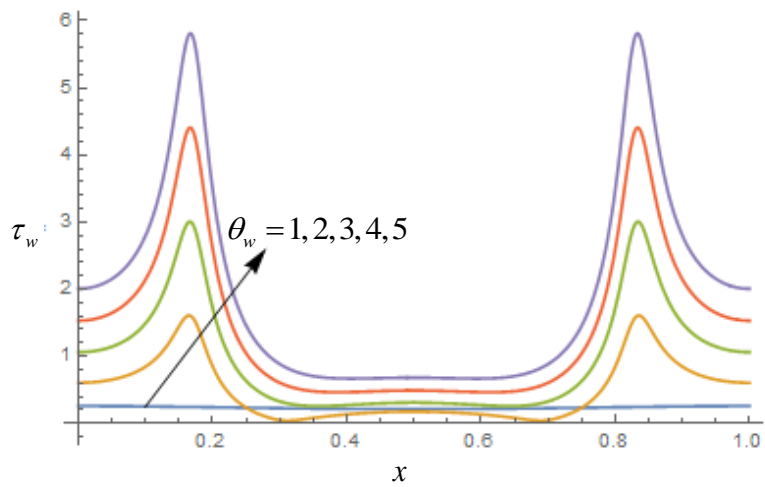


Figure 26: Effect of θ_w values on Shear Stress along the stenosed region

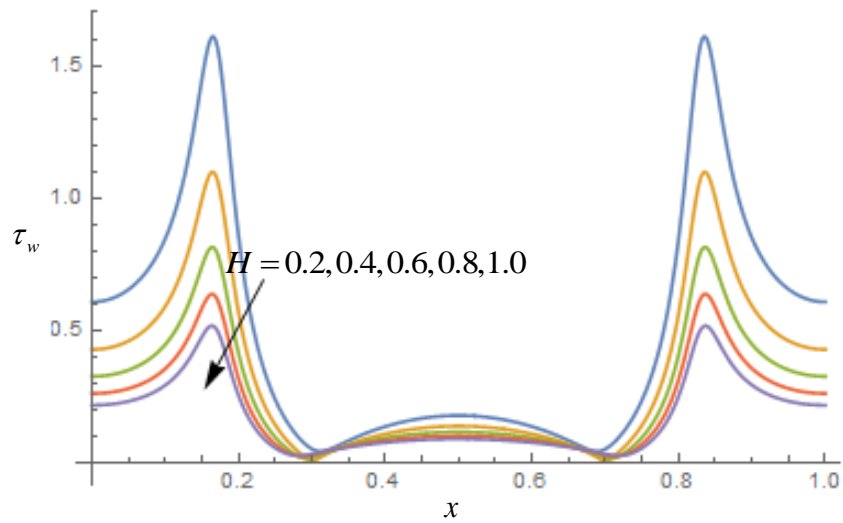


Figure 27: Effect of H values on Shear Stress along the stenosed region

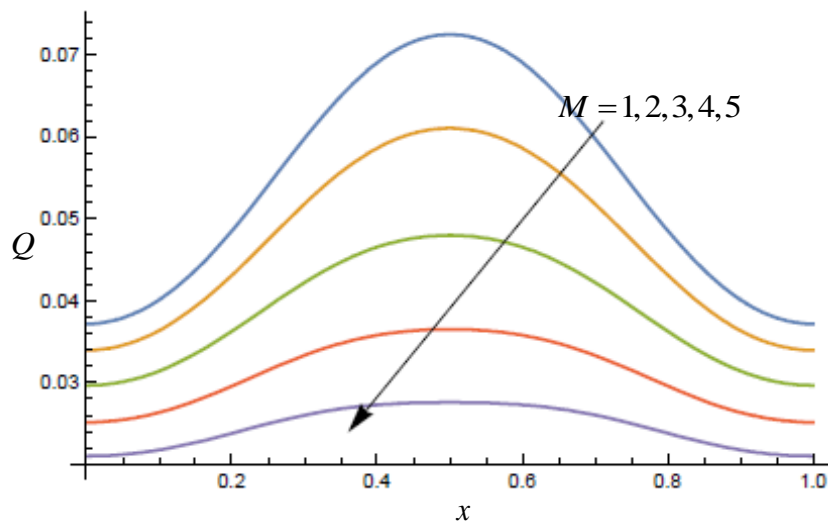


Figure 28: Effect of M values on Flow Rate along the stenosed region

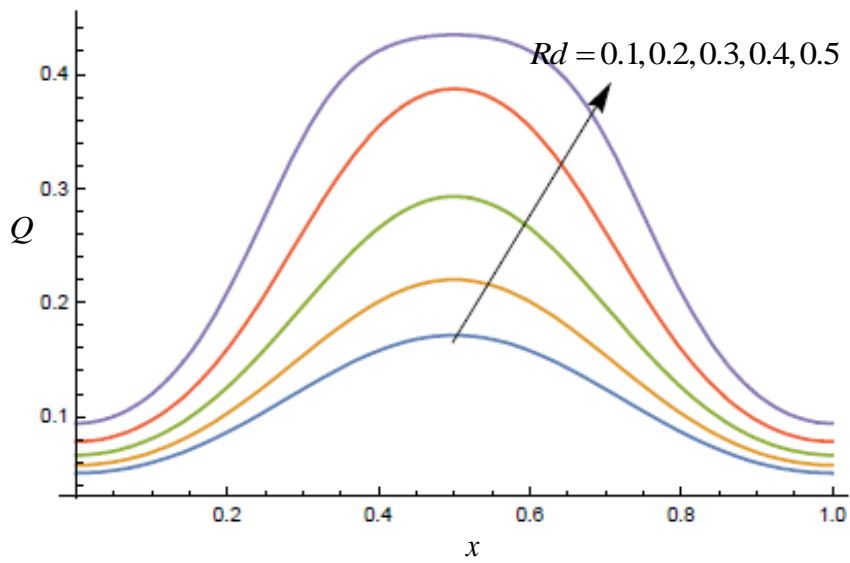


Figure 29: Effect of Rd values on Flow Rate along the stenosed region

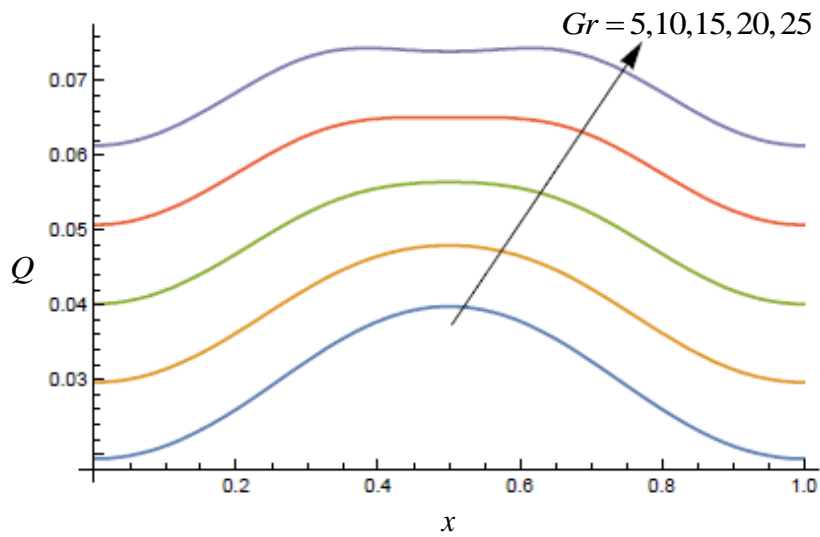


Figure 30: Effect of Gr values on Flow Rate along the stenosed region

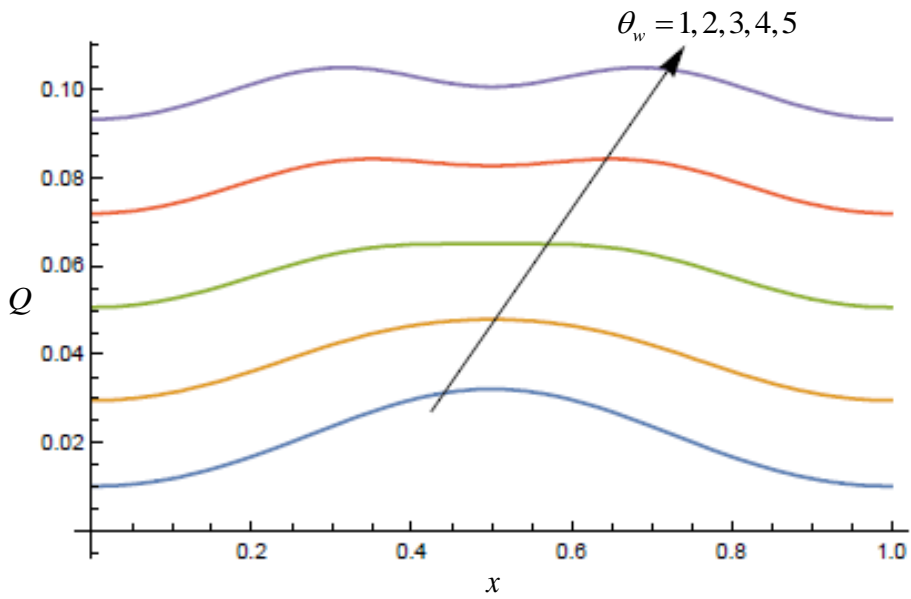


Figure 31: Effect of θ_w values on Flow Rate along the stenosed region

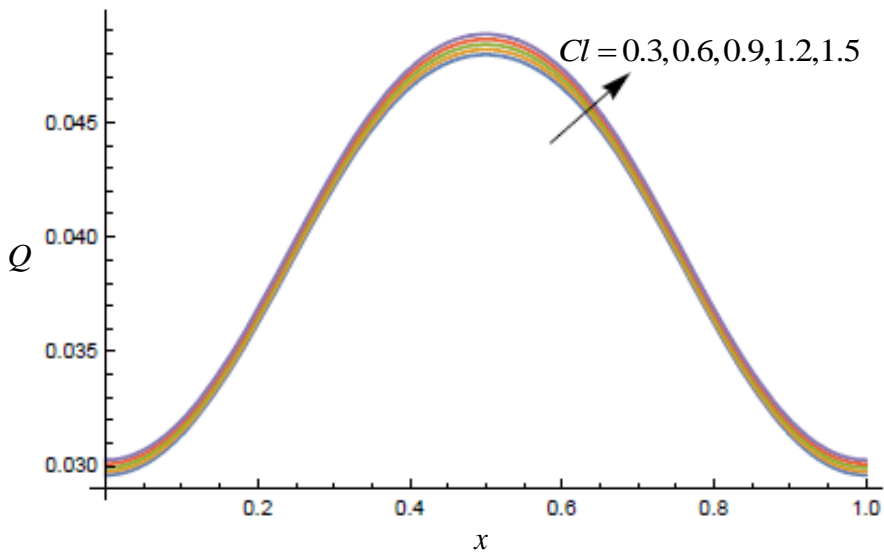


Figure 32: Effect of Cl values on Flow Rate along the stenosed region

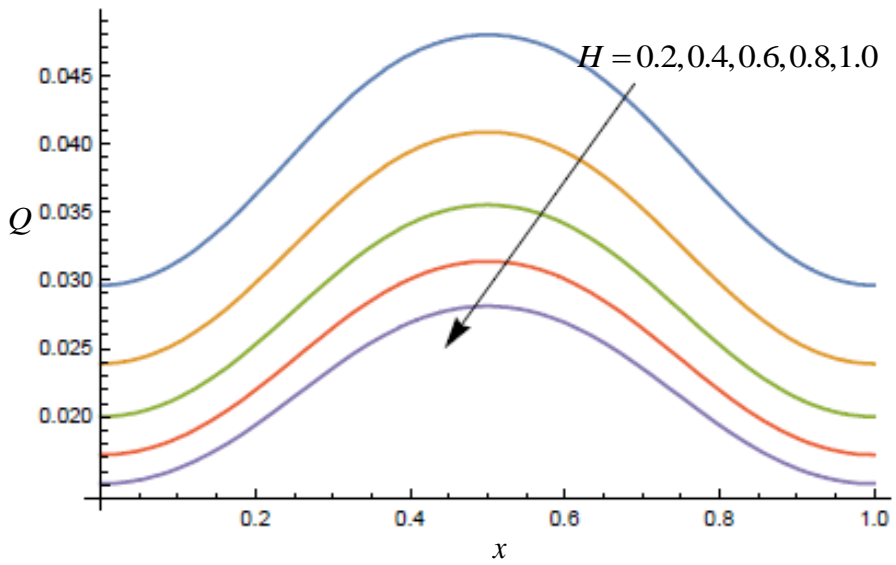


Figure 33: Effect of H values on Flow Rate along the stenosed region

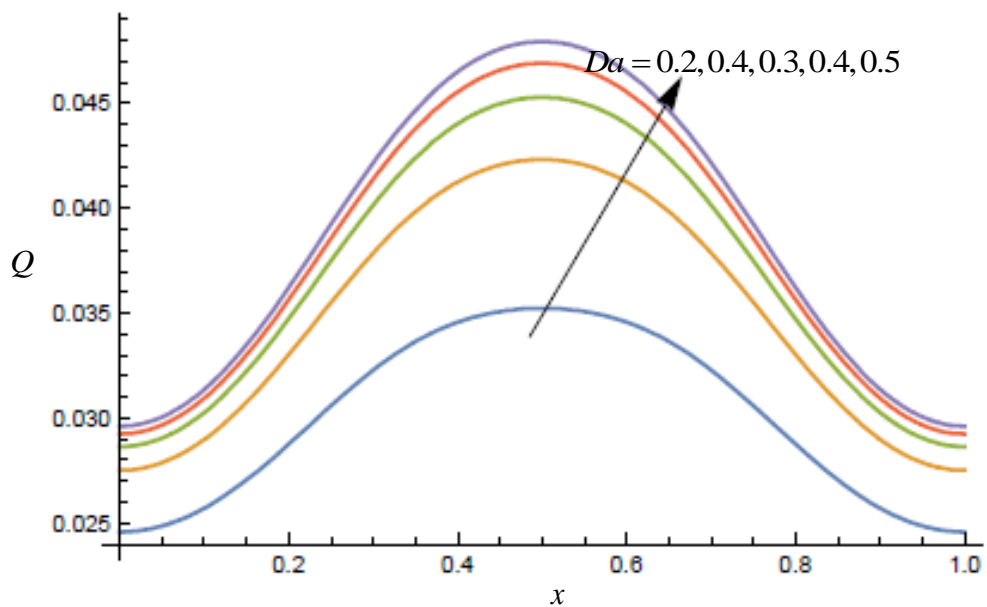


Figure 34: Effect of Da values on Flow Rate along the stenosed region

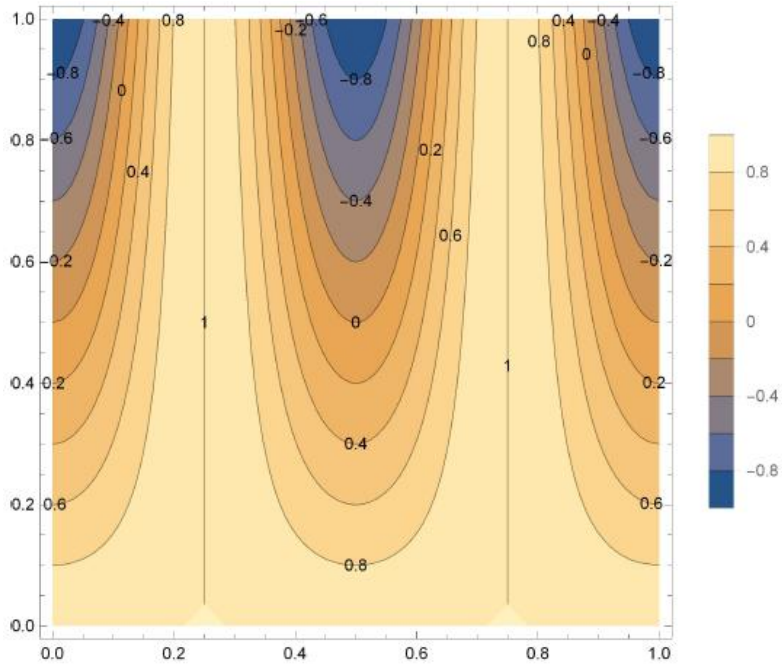


Figure 35: Contour plot showing the tumor δ along the horizontal distance

5. Discussion of results

This section deals with the discussion of the graphical results presented as Figure 1 to Figure 36 in the above sections. The discussions are as follows:

Figure 1 shows the influence of the Darcy number on velocity profile with other pertinent parameters:

$\theta_w = 1, Rd = 3, Pr = 21, M = 3, Cl = 0.3, Gr = 10, H = 0.2, \delta = 0.3, R_T = 1.2, \alpha = 0.3$ and $x = 0.3$.

It is seen that velocity profile increases as a result of increase in porosity. This result is in agreement with existing physical laws. The wall temperature influence was also been investigated in our simulation, and it is noticed in **Figure 2** that the wall temperature increase, increases the velocity of the blood in the tissue.

This is so because external heating is applied to constricted tissue to heat up the area and aid blood circulation with the support of the other parameters:

$$Da = 0.05, Rd = 3, Pr = 21, M = 3, Cl = 0.3, \quad Gr = 10, H = 0.2, \quad \delta = 0.3, R_T = 1.2 \\ \alpha = 0.3 \text{ and } x = 0.3.$$

Figure 3, illustrates the influence of radiation on velocity profile, it is seen that the velocity profile increase when radiation increases. This result is the fact that increase in radiation results to a decrease in blood viscosity and that in turn results to thinning of the blood and improve in circulation with other pertinent parameter values as in the preceding discussion. **Figure 4**, shows the influence of the perfusion parameter on velocity profile while other pertinent parameters are kept moderate. In that result, we noticed that the velocity profile increase to a peak before decelerating to zero, but for increase in perfusion parameter values decreases the velocity profile of the fluid flowing through the channel. **Figure 5**, depicts a velocity profile with increasing values of magnetic field intensity. The figure shows that velocity profile decrease as magnetic field intensity increases, and this result is the fact when a magnetic field is applied to moving electrically conducting fluid such as blood, it generate a force called the Lorentz force, which opposes the flow. The Grashof number influence on blood velocity in the tissue is shown in **Figure 6**, the figure shows an increase in blood velocity as the Grashof number increases. The importance of haematocrit was investigated and presented in **Figure 7**, and the figure shows that increase in haematocrit decreases the blood flow because of the fact the increase could result to more dense fluid and inhibit blood circulation. The height of stenosis is a serious circulatory disorder in human, as seen in **Figure 8**. The figure shows that increase in stenosis height causes a decrease in blood circulation because it narrows the circulatory channel. The idea of the treatment is to find a way of having a control of circulatory challenges as figured in **Figure 9**. This figure is of the view that application of treatment to flow challenge could improve the circulation, even though not too huge. **Figure 10**, shows the influence of womersley number on blood velocity; it is seen that increase in the parameter decreases the velocity of blood. **Figure 11 and Figure 12** shows the influence of wall temperature and radiation parameter on blood velocity, it is noticed that there is a temperature increase as a result of the wall temperature and radiation parameter increase. These results agree with basic law of physic in the area of heating up and exciting the molecules around the tumor in order to aid heat circulation for deep heat treatment. The implication of perfusion rate is elucidated in **Figure 13**, and the figure shows a decrease in temperature profile as the perfusion rate decreases. Increase in tumor/stenosis adversely affects the temperature profile as seen in **Figure 14**. This figure shows that the temperature profile decrease as the tumor gets bigger. This is a common scenario because of the proliferation rate of tumor, which is more than normal tissue. The influence of tumor treatment was also investigated with result shown in **Figure 15**, the figure shows that under normal consideration

as presented in this research the treatment increase resulted to the temperature profile increase. **Figure 16**, illustrates that increase in womersley number decreases the temperature profile. The rate of heat transfer was investigated and results presented in **Figure 17 – Figure 22**. The figures show that increase in $\theta_w, Rd, Cl, \omega, \delta$ increases the rate of heat transfer with other pertinent parameters taken as in Figure 1. But increase in the treatment parameter decreases the rate of heat transfer in **Figure 22**. Investigation of wall shear stress was presented in **Figure 23 – Figure 27**. **Figure 23 – Figure 26** show an increase in wall shear stress as a result of the increase in M, Rd, Gr and θ_w with other pertinent parameters as seen in figure 1, while the shear stress decreases as a result of the increase in haematocrit H values. Finally, the volumetric flow rate was investigated as presented in **Figure 28 – Figure 34**. **Figure 28** and **Figure 33** show a decrease in volumetric flow rate as the magnetic field intensity and haematocrit values increases, while the increase in radiation parameter, Grashof number, wall temperature parameter and Darcy number and perfusion rate increases the volumetric flow rate. **Figure 35** shows the contour result of geometry of the tumor as the height grows along different location.

6. Conclusion

Theoretical investigation of the role of perfusion rate and haematocrit on blood flow and its impact on radiation behavior of tissue for tumor treatment was carried out with presentation of the governing models in equations (1) and (2). The analytical solutions were simulation with resulted pertinent parameters varied within a specific range to study their significant. Graphical results were presented and discussions done all in the preceding sections, and we conclude as follows:

- (a) The blood velocity increases with an increase in Darcy number, wall temperature parameter, radiation parameter, Grashof number and the treatment parameter, which are very helpful in deep heat treatment, while perfusion rate, haematocrit parameter, height of stenosis and womersley number parameters increase decreases the blood velocity profile.
- (b) The wall temperature parameter, radiation parameter and treatment parameter increases the temperature profile of the fluid while the perfusion rate, height of stenosis, and womersley number decreases the temperature profile of the fluid.
- (c) The wall temperature parameter, radiation parameter, perfusion rate, oscillatory frequency parameter and height of stenosis increase the rate of heat transfer, while the treatment parameter decreases the rate of heat transfer.

- (d) The magnetic field intensity, radiation parameter, Grashof number, and wall temperature parameters values increases the rate of wall shear stress, while the haematocrit parameter values decreases the rate of wall shear stress.
- (e) The radiation parameter, Grashof number, Darcy number, wall temperature parameter and perfusion rate increases the volumetric flow rate, while the magnetic field intensity and haematocrit parameters decreases the volumetric flow rate.

In order to treat patients more accurately with the aim of getting a better results in thermal therapy for relieving pain. The study gives better understanding of the thermal processes and the contribution of perfusion rate and haematocrit during blood circulation. The study will also be of interest to clinicians who are involved in the treatment of cancer and tumors by using the method of electromagnetic hyperthermia. This technique involves overheating the affected tissues up to 42°C. The study also finds applications in estimating the electromagnetic radiation when humans has to work in radiation fields, for the fact that the study considered heat transfer and performing heat dose sensitivity tests, which is required for using the method of hyperthermia in an appropriate matter.

References

- [1] Higashi, T., Yamagishi, A., Takeuchi, T., Kawaguchi, N., Sagawa, S., Onishi, S. and Date, M., (1993). Orientation of Erythrocytes in a strong static magnetic field, *J. Blood*. 82(4), 1328-1334.
- [2] Chandrasekhar, S.(1961). *Hydrodynamic and Hydro magnetic Stability*, Oxford University Press London.
- [3] Rudraiah, N. (1962), Magnetohydrodynamic stability of heterogeneous incompressible non-dissipative conducting liquids, *Appl. Sci. Res.*, 11, 105-117.
- [4] Haik, Y.,Pai, V. and Chen, C.J., (1999). Development of magnetic device for cell separation, *J. Magn. Mater.*, 194, 261.
- [5] Ruuge, E.K. and Rusetski, A.N. (1993), Magnetic fluid as drug carriers: Targeted transport of drugs by a magnetic field,, *J. Magn.Magn.Mater*, 122, 335.
- [6] Misra, J.C. and Shit, G.C. (2007), Effect of Magnetic field on blood flow through an artery: A numerical model, *Tom.*, 12(4), 3-16.
- [7] Chaturani, P. and Kaloni, P.N., (1976), Two-layered poiseuille flow model for blood flow through arteries of small diameter and arterioles, *Biorheology*, 13, 243-250.
- [8] Chaturani, P. and Upadhya, V.S., (1979), A two-layered model for blood flow through small diameter tubes, *Biorheology*, 16, 109-118.
- [9] Shukla, J.B., Parihar, R.S. and Gupta, S.P. (1980), Effects of peripheral layer viscosity on blood flow through the artery with mild stenosis, *Bull.Math. Biol.*, 42, 797-805.
- [10] Chaturani, P. and Biswas, D., (1983), A theoretical study of blood flow through stenosed arteries with velocity slip at the wall, *Proc. First Internat. Symposium on Physiological Fluid Dynamics*, IIT Madras, India, 23-26.
- [11] Majhi, S.N. and Usha, L., (1984), Fahraeus-Lindqvist effect and generalized poiseuille flow with or without wall slip, *Proc. 13th Nat. Conf. Fluid Mech. Fluid Power*, REC, Thiruchirappalli, India, 125-128.
- [12] Philip, D. and Peeyush Chandra (1996), Flow of eringen fluid(simple micro fluid) through an artery with mild stenosis, *Int. J. Eng. Sci.*, 34, 87-99.
- [13] Tzirtzilakis, E.E., (2005), A Mathematical model for blood flow in a magnetic field, *Physics of Fluids*
- [14] Ramakrishnan, K. and Shailendhra, K. (2011), Hydromagnetic flow through uniform channel bounded by porous media, *Appl. Math. Mech.-Engl. Ed.*, 32(7), 837-846.
- [15] Rudraiah, N. (1985), Coupled parallel flows in a channel and a bounding porous medium of finite thickness, *Trans. ASME* . 107(3), 322-329.
- [16] Rudraiah, N., Chiu-on Ng, Nagaraj, C. and Nagaraj, H.N., (2006), Electrohydrodynamic dispersion of Macromolecular components in biological bearing, *Journal of Energy, Heat and Mass transfer*, 28, 261-280.

- [17] Rudraiah, N., Chiu-on Ng and Nagaraj, C., (2007), Electrohydrodynamic dispersion of Macro- molecular components in biological bearing Effect of Artificial cartilage made up of smart material of nanostructure on dispersion in poorly conducting macromolecular components in synovial joints, *Key Engineering Materials*, 334-335, 1245-1248.
- [18] Ng, C.O., Rudraiah, N. and Nagaraj, C. (2008), Electrohydrodynamic pulsatile flow in a channel bounded by porous layer of smart material, *Int. J. Engg. Sci.*, 5, 1-13.
- [19] Shivakumar, P.N., Nagaraj, S., Veerabhadraiah, R. and Rudraiah, N. (1986), Fluid Movement in a channel of varying gap with permeable walls covered by porous media, *Int. J. Engng. Sci.*, 24(4), 479-492.
- [20] Misra, J.C. and Chakravarty, S. (1986), Flow in arteries in the presence of stenosis, *J. Biomech.*, 19, 907-918.
- [21] Copley, A.L., (1990). Fluid mechanics and rheology, *Biorheology*. 27, 3-19.
- [22] Bunonyo, K.W., Israel-Cookey, C. and Amos, E., 2017. MHD Oscillatory Flow of Jeffrey Fluid in an Indented Artery with Heat Source. *Asian Research Journal of Mathematics*, pp.1-13.
- [23] MacDonald, D.A. (1974), *Blood flow in arteries*, 2nd ed., London: Edward Arnold Publishers.
- [24] Burton, A.C., (1966), *Physiology and Biophysics of the Circulation*, Introductory Text, Year Book Publisher, Chicago.
- [25] Valvano JW, Nho S, Anderson GT (1994), Weinbaum-Jiji moel of blood flow in canine kidney cortex for self-heated thermistorsrom. *J Biomech Eng* 116:201-207.
- [26] Chato JC (1980), Heat transfer to blood vessels. *J Biomech Eng* 102:110-118.

NOMENCLATURE

w^*	Dimensional velocity profile
w_0	Perturbed velocity profile
x^*, y^*	Dimensional distances
R	Radius of an abnormal tissue
R_0	Radius of normal tissue
R_T	Treatment parameter
H	Haematocrit parameter
δ	The height of tissue growth
d_0	Onset of tumor
α	womersley number
Rd	Heat absorption constant
k_b	Thermal conductivity of blood
Da	Darcy number
Gr	Thermal Grashof number
W_b	The rate of blood perfusion
Cl	Perfusion parameter
C_b	The specific heat capacity of blood
B_o	Strength of applied magnetic field
c_p	Specific heat capacity at constant pressure
Pr	Prandtl number for blood
M	Magnetic parameter
T_a^*	Temperature of blood
T_t^*	Temperature of the fluid far from the plate

Greek Symbols

ν	Kinematic viscosity of blood
μ	Dynamic viscosity of blood
g	Acceleration due to gravity
λ	Length of tumor
ω	Oscillatory frequency
θ	Dimensionless temperature
θ_o	Dimensionless perturbed temperature
θ_w	Wall temperature of blood
ρ	Density of the fluid